1. Amier Hafizun Ab. RASHID[1], **2. Badrul Hisham AHMAD**[1] **3. Mohamad Zoinol Abidin ABD AZIZ**[1], **4. Nonikman HASSAN**[1], **5. Mazlee MAZALAN**[2]

[1]Universiti Teknikal Malaysia Melaka (UTeM), Faculty of Electronics and Computer Engineering (FKEKK),
Centre for Telecommunication Research and Innovation (CeTRI)
[2]Universiti Malaysia Perlis, Micro System Technology, Centre of Excellence (CoE),
ORCID: 1. 0000-0002-3203-7567, 2. 0000-0001-8014-2444, 3. 0000-0002-9926-158X, 4. 0000-0003-1465-9634, 5. 0000-0002-4946-2893

Parametric Studies of CPW Pentagonal Sierpinski Gasket Fractal Patch Antenna

Abstract . *The parametric study on a dual band CPW Pentagonal Sierpinski gasket fractal patch antenna for WiMAX and WLAN applications is presented in this work. In order to accomplish and advantages of multi-band, broadband, high gain, and low-profile antennas, novel geometries must be developed due to the limits of the conventional antenna design, Sierpinski gasket fractal structure is chosen to improve the antenna performance. The work began with Antenna A as the initiator step with pentagonal patch with CPW technique. Then, it goes with Antenna B was the first iteration stages with pentagonal slot. After that, the work continued by five different parametric studies are chosen in this work to define the effect of different dimensions of the patch antenna. The first and second parametric study works include a different width and length size of the patch antenna at Antenna A. The other three involved in the Antenna B, are including the different dimensions of the CPW / feeding antenna gap, feed line, and lastly the slot width dimension. At 3.5 GHz and 5.8 GHz, the antenna's aimed frequencies are - 31.70 dB and - 22.00 dB, respectively, and these values are feasible for WiMAX and WLAN operation.*

Streszczenie . *W pracy przedstawiono badanie parametryczne dwuzakresowej anteny CPW Pentagonal Sierpińskiego z uszczelką fraktalną dla aplikacji WiMAX i WLAN. Aby osiągnąć i wykorzystać zalety anten wielopasmowych, szerokopasmowych, o dużym zysku i niskoprofilowych, należy opracować nowe geometrie ze względu na ograniczenia konwencjonalnej konstrukcji anteny, wybrano strukturę fraktalną uszczelki Sierpińskiego w celu poprawy wydajności anteny. Pracę rozpoczęto od Anteny A jako kroku inicjującego z pięciokątną łatą techniką CPW. Następnie, z anteną B, były pierwsze etapy iteracji z pięciokątną szczeliną. Następnie w tej pracy wybrano pięć różnych badań parametrycznych, aby określić wpływ różnych wymiarów anteny krosowej. Pierwsze i drugie badania parametryczne obejmują różne wymiary szerokości i długości anteny krosowej na antenie A. Pozostałe trzy prace związane z anteną B obejmują różne wymiary szczeliny CPW/anteny zasilającej, linii zasilającej i wreszcie wymiar szerokości szczeliny. Przy 3,5 GHz i 5,8 GHz docelowe częstotliwości anteny wynoszą odpowiednio -31,70 dB i -22,00 dB i wartości te są możliwe do pracy w sieciach WiMAX i WLAN. (**Badania parametryczne pięciokątnej fraktalnej anteny krosowej CPW z uszczelką Sierpińskiego)*

Keywords: Fractal Geometries, Patch Antenna, Sierpinski Gasket, Coplanar Waveguide, Return Loss
Słowa kluczowe: Geometrie fraktalne, antena łatek, uszczelka Sierpinski, falowód współplanowy, badania parametryczne

Introduction

Due to the design restrictions, manufacturing challenges, and technical developments, the fractal antenna design has become a constraint for some researchers [1]. Besides that, the usage of antennas with a broad bandwidth [2], higher efficiency, and robustness is currently required for the wireless communication systems. Most of the basic antennas are often shown a narrowband characteristic. The physical size of the antenna depends on the frequency. The most recent and ongoing developments technique in the wireless communication application give an impact on the design of multifunctional antennas with the multiband capability such as using metamaterial structure [3], Multiple-Input Multiple-Output (MIMO) [4] or using fractal structure.

Hence, to provide a dual-band frequency resonance for 3.5 GHz WiMAX and 5.8 GHz WLAN applications, the ideal choice is a small size of a planar antenna. This is due to the facts that there is a need for the small size and lightweight wireless communication devices to produce an efficient, unobtrusive, and economical patch antenna to the users in which all parts of nature exhibit the fractal patterns. Antennas are one of the numerous scientific and engineering sectors that has been significantly impacted by the fractal geometry. Thus, some of these forms are already available as commercially useable antennas for various telecommunications applications.

Due to the antenna limitless of a single frequency, fractals are abstract objects that are satisfying in the strict sense of mathematical description but cannot be physically constructed. However, there are other implications that can be done on fractals that make it possible to develop an electromagnetic device, such as antennas [4]. Both surface antenna and the linear elements size can be reduced using the fractal structures [5-6]. Similarly, the length of wire used to expand the electrical dimensions of flat radiating elements can be reduced as well. In 1977, Mandelbrot [7] developed the basic theory of fractal geometry. Fractal geometries are the structures that may be divided into the equal, straightforward parts, better matching of input impedance, and reduce mutual coupling in an antenna array [8]. Fractals are geometric objects with geometric dimensions that vary from fractal dimensions and are self-similar at various sizes. As a result, the fractal geometric shape has advantages over the conventional forms of antennas, including a resonant frequency tunable, antenna size reduction, and multiple resonance frequencies.

In the field of microwave engineering, these fractal geometries are now used to create several types of microwave applications, including antennas, frequency selective surfaces, image processing, and biomedical signal processing. The usage of an iteration function system with comparable shapes is made possible by the self-similarity aspect of the fractal geometry. The Sierpinski gasket [9], Minkowski curve [10], Von-Koch snowflakes [11], Hilbert curve [12], hexagonal fractal shaped [13], and others are examples of the fractal geometry in the antenna design.

An initiator and a generator are used repeatedly in the creation of fractal structures. A crucial component of the fractal structure representation is the self-similarity dimension (Ds), which is provided by Equation 1 [14]:

(1) $$D_s = \log(N) / \log(r)$$

Where, N is the overall number of replicas that are self-similar; r represents the scale factor of self-similarity dimension; An integer is not required for the D_s

The fourth iteration of numerous fractal structures' initiator and generator concept and sample is shown in Figure 1 [15]. A generator is a compiled set of scaled-down versions of the initiator for Koch Curve. Starting with a straight line in the first step and after that, it needs to be divided into three equal parts and the middle part needs to be replaced with two sides of an equilateral triangle that are the same length as the section that is being removed. This is followed by substituting each of the middle segments with two sides of an equilateral triangle, splitting each of the four resulting segments into three equal halves, and repeating the process for all four segments.
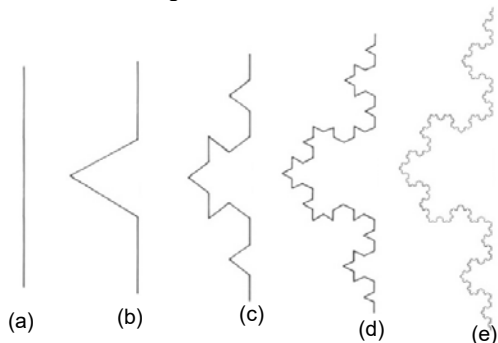
Fig. 1: Example of iteration stage of the Koch Curve fractal structures, (a) initiator (zero iteration), (b) first iteration, (c) second iteration, (d) third iteration, (e) fourth iteration [15]

It substitutes each line segment with the spiking shape displayed in the generator at each iteration step of Koch Curve. This idea is displayed in Figure 2 [16].
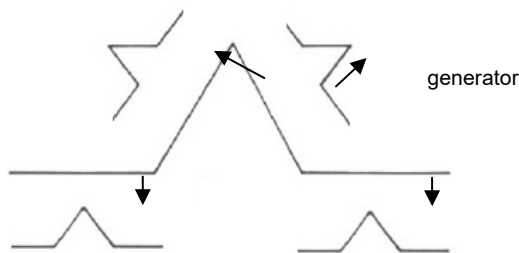

Fig. 2. Spiking shape fractal [16]

The Sierpinski triangle or gasket was first demonstrated in 1916 by a Polish mathematician. Puente then created the Sierpinski gasket-inspired fractal multiband antennas in 1996 [17], which had five unique heights and a factor of two between scales. Additionally, a variety of Sierpinski gasket designs were applied to the antenna in order to enhance its functionality of multiband. For getting many bands, a modified Sierpinski fractal antenna was developed. To accomplish the wideband response, some antenna dimensions were tuned asoptimization process. The zero-iteration design, often referred to as the initiator, or the first design stage in the Sierpinski gasket structure. The next step is to apply the first iteration process and followed by the second iteration process. The scale factor of Equation 2 was used, which may be calculated as follows:

(3) $$scale\ factor = \frac{F_R(n+1)}{F_R(n)}$$

Where, F_R is the resonant frequency, n is the iteration number

The resonant frequency of a Sierpinski gasket can be calculated by using the formula in Equation 3 [14].

(3) $$f_r = K \frac{C}{L} cos\frac{\alpha}{2} \delta^n$$

where, f_r Frequency Fractal, δ Scale factor, K iteration, n Band number, Velocity C, length L.

The Sierpinksi iteration development stage; comprising the triangular and square shapes, is depicted in Figure 3 [18].
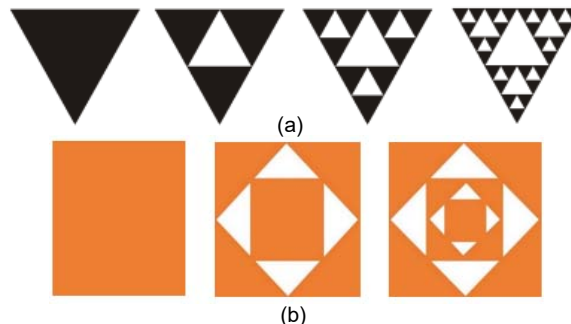

Fig. 3: The Sierpinski iteration development stage, (a) triangular [18], (b) square

Many researchers use the Sierpinski gasket structure to enhance the antenna performance as reported in the past literature review. Devcsh [19] had implemented a Rotated Square Sierpinski Gasket (RSSG) on the antenna to produce multiple resonance frequencies of at 6.95 GHz, 15.77 GHz, 18.24 GHz, 20.91 GHz, and 25.63 GHz for C-band, Ku band, and K-band applications, respectively. Additionally, Chaouche [18] has developed a modified Sierpinski Gasket with a hexagonal-shaped for multiband operation at 1.6-1.7 GHz (L-band), 1.71-1.88 GHz (DCS), 1.85-1.95 GHz (PCS/TD-SCDMA/LTE), 5.2/5.8 GHz (Wireless Local Area Networks (WLAN)), and 10 GHz (X-band applications).

Franciscatto [21] in his work introduced the Sierpinski fractal shape antenna (reader) with high gain for RFID applications at 868 MHz. The measured return loss and gain are – 16.0 dB and 16.4 dB, respectively while the measured radiation efficiency is greater than 92 % with. Furthermore, there are several works that apply the Sierpinski gasket structure to improve the antenna performance which also have been reported [22-25].

Other research on the Sierpinski gasket fractal antenna has been done in the past, such as Remya's [26] octagonal Sierpinski fractal antenna, which improves the bandwidth operation ranged at MBAN (2.362 GHz – 2.4 GHz) and ISM frequencies (2.4 GHz – 2.48 GHz) with 1.23 GHz bandwidth, and return loss of – 26.86 dB at 2.41 resonating frequency. The superstrate cross slot adopted in the Sierpinski Carpet antenna shows the gain improvement of 4.67 dB and 7.4 dB at 3.5 GHz and 5.6 GHz [27]. improved gain characteristic of 4.67 dB and 7.4d B, respectively. Several parametric studies had been taken into consideration for the comparison in this work.

In this paper, the fractal antenna design is based on the pentagon shape for a dual-band application. The second stage iteration is adopted using the Sierpinski Gasket design technique. Due of its outstanding broadband performance, the Sierpinski gasket antenna is essential in research. The antenna is targeted for WiMAX and WLAN applications.

Antenna Design

The antenna is designed step-by-step, starting with the basic design antenna patch. Antenna A, which has the

design of a basic patch of the pentagonal shape. Then it moves to the next design of Antenna *B*, consisting of the first iteration of the fractal design.

Fractal Geometry Design

Mathematical sets defined as fractals often result from the recursion and have the fascinating dimensional features. A repeating disposition of self-similar objects during each iteration phase is the self-similarity property of the fractal geometry design. Figure 4 depicts an example of the pentagonal Sierpinski gasket's development process, from the initiator or zero iteration design to the first and second iterations. The concept is to apply the cut out same pentagonal slot shaped in the middle of the patch but with smaller size. The scale and dimension of the fractal geometry are determined at a distinct stage of design.
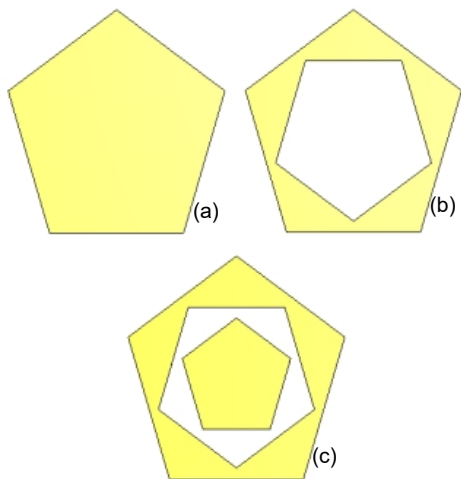
Fig.4. Proposed pentagonal Sierpinski gasket development stage, (a) initiator / zero iteration, (b) first iteration, (c) second iteration

Antenna Design

Basic Antenna A, which has a patch with the pentagonal form; and Antenna B, which has a patch with the pentagonal slot, are the two stages of development of the antenna. The simulation software CST Microwave Studio is used to create both designs. Several antennas will be employed in a later stage of this work to compare various parametric research dimensions. Its performance will be compared across the five key aspects.

The first piece of work is the antenna, which is made of copper that is 0.035 mm thick and is mounted on a FR4 substrate that is 1.6 mm thick and has a dielectric constant of 4.3. It has a substrate, a coplanar waveguide (CPW) structure, a patch with the pentagonal form, and a feeding line that connects to the antenna source (waveguide). The fundamental pentagonal antenna construction of Antenna A is shown in Figure 5. It shows that the antenna measures 25.2 mm in width and 25.1 mm in length, respectively.
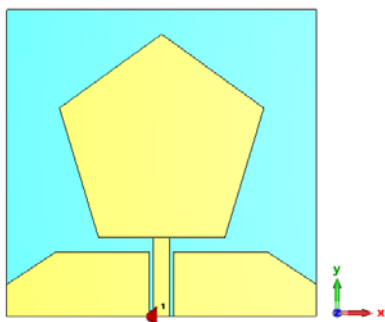
Fig. 5. Basic pentagonal antenna structure with CPW of Antenna *A*.

In addition, Figure 6 represents the Sierpinski gasket fractal iteration concept of first iteration stages; the simulation and the fabricated of the proposed antenna B. The SMA connector is connected to the antenna at the feed line. There are no copper plate at the back part because the ground at CPW is located at the front part that connected by SMA connector.
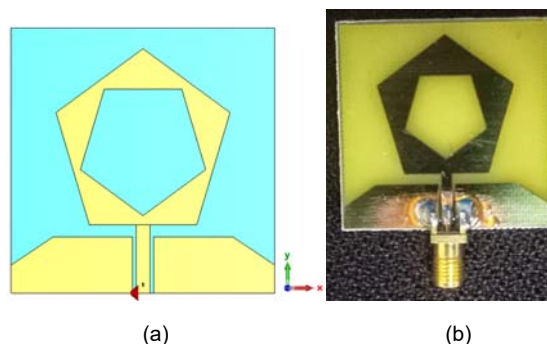
(a)   (b)

Fig. 6. CPW Pentagonal Sierpinski Gasket fractal patch antenna of Antenna *B*, (a) simulation and (b) fabricated version.

Table 1: CPW Pentagonal Sierpinski Gasket fractal patch antenna of Antenna *A* and Antenna *B*

Parameter of the antenna	Symbol	Dimension (mm)	
		Antenna *A*	Antenna *B*
Substrate width	W_s	38	38
Substrate length	L_s	38	38
Patch width	W_p	25.07	25.07
Patch length	L_p	25.19	25.19
Feed line width	W_f	2	2
Feed line length	L_f	9.8	9.8
CPW width	W_c	17.5	17.5
CPW length	L_c	8	8
Substrate thickness	T_s	0.035	0.035
Slot width	W_{slot}	-	18.04
Slot length	L_{slot}	-	18.13
Feedline gap	G_f	0.5	0.5

Result

The gain in GHz (dB versus frequency), return loss in GHz (dB versus frequency), and the antenna's bandwidth and radiation pattern performance are among the proposed antenna parameters that are explained in this section. For resonance frequency, this proposed antenna must transmit and receive at least 90 % of the signal.

The return loss of Antenna A is depicted in Figure 7 with various patch length dimensions. It demonstrates how increasing the patch length dimension has an impact on the performance of the return loss at the initial resonant frequency. Patch length = 20.2 mm, for instance, results in -16.15 dB at 3.88 GHz, whereas patch length = 27.7 mm yields - 25.24 dB at 3.37 GHz.

However, the length increase has a tendency to lessen return loss performance at the second resonant frequency. As an illustration, a patch length of 20.2 mm results in a - 40.78 dB at 6.09 GHz whereas a patch length of 27.7 mm produces a - 21.08 dB performance at 5.88 GHz. In addition, it is evident that the resonant frequency at both the first and second resonant frequencies had been moved to the left point of the result.
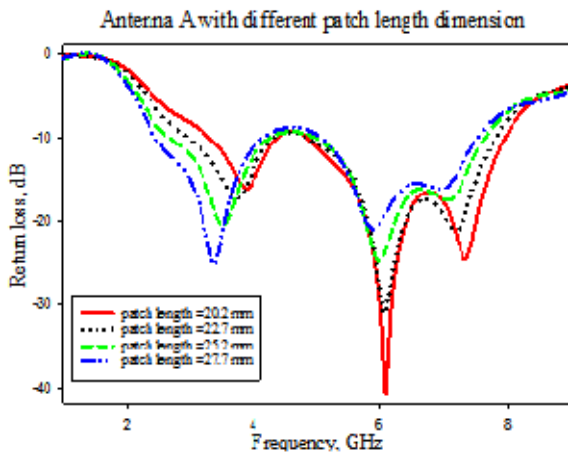
Fig. 7. Return loss of Antenna A with different patch length

Figure 8 depicts the return loss performance of Antenna A with various patch width dimensions. It shows that the increment of the patch width dimension effect to reduce the return loss performance at the first resonant frequency. For example, patch length = 20.1 mm effect to – 46.67 dB at 3.68 GHz while patch length = 27.6 mm with only performance of – 16.39 dB at 3.55 GHz. It also shown the patch length = 20.1 mm create three resonant frequencies at 3.68 GHz, 5.96 GHz, 7.70 GHz with -46.67 dB, - 29.12 dB and - 42.46 dB while patch length = 27.6 mm shown only at two-point 3.55 GHz and 6.09 GHz with – 16.39 dB and – 21.13 dB, respectively.
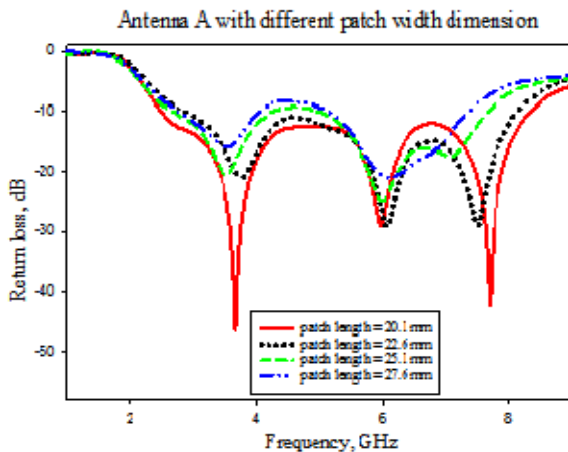

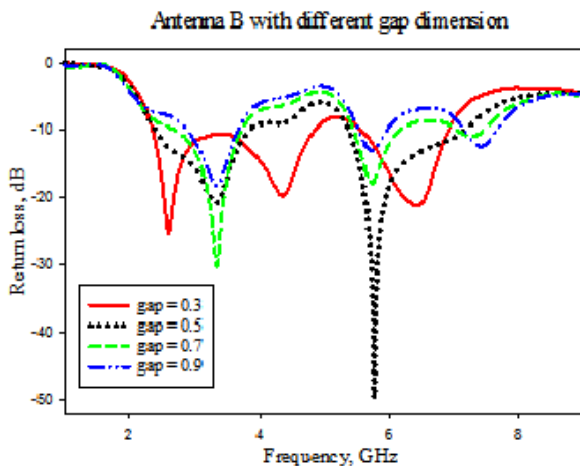Fig. 8. Return loss of Antenna A with different patch width

Fig. 9. Return loss of Antenna B with different feedline and CPW gap dimension

Next, Figure 9 represents the return loss of Antenna B with different gap dimension between feedline and CPW structure starting from 0.3 mm to 0.9 mm. For gap = 0.5 mm effect to resonates at dual frequency at 3.32 GHz with – 20.823 dB and 5.768 GHz with – 49.62 dB. It shows that the increasing the gap from 0.5 mm to 0.7 mm and 0.9 mm will effect to reduce the resonant frequency at the second resonant frequencies. It also shows that the results of – 18.24 dB and – 13.26 dB at 5.72 GHz and 5.73 dB for gap = 0.7 mm and 0.9 mm, respectively.

Next, Figure 10 shows the return loss of Antenna B for various feedline to CPW structural gap sizes ranging from 0.3 to 0.9 mm. At dual frequencies of 3.32 GHz with - 20.823 dB and 5.768 GHz with - 49.62 dB, the effect resonates for a spacing of 0.5 mm. It demonstrates how widening the distance from 0.5 mm to 0.7 mm and 0.9 mm will cause the second resonant frequencies to become less resonant. Additionally, it demonstrates the values of - 18.24 dB and - 13.26 dB at 5.72 GHz and 5.73 dB, respectively, for gap = 0.7 mm and 0.9 mm.
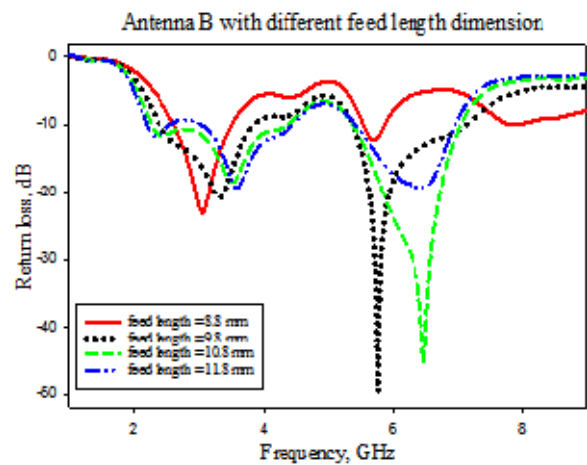

Fig. 10. Return loss of Antenna B with different feedline length

Furthermore, Figure 11 displays the return loss performance for Antenna B with a range of slot widths, from 12.6 mm to 18.0 mm. It demonstrates the slightly varying return loss performance values at the initial resonance frequency point. In this instance, slot width = 12.6 mm exhibits the worst return loss value of - 21.02 dB at 3.29 GHz, whereas slot width = 18.0 mm exhibits the performance of - 26.79 dB at 3.47 GHz. On the opposite side of the second resonant frequency, the slot width = 12.6 mm performs poorly at 5.99 GHz, with a return loss value of -29.24 dB, whereas the slot width = 18.0 mm performs well at 5.74 GHz, with a return loss value of -49.33 dB.
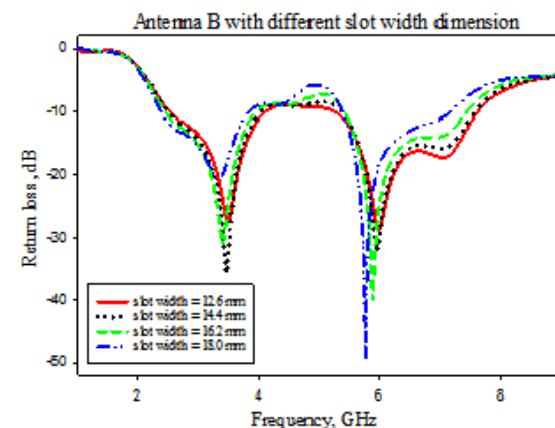

Fig. 11. Return loss of Antenna B with different slot width

Figure 12 compares the measurement of Antenna *B* to its modelling. The effectiveness of Antenna *B* is then specifically compared utilising the outcomes of simulation and measurement. The shifting point of the resonant frequency exhibited a lower discrepancy in the measurement as compared to the modelling results. The measurement shows that it has operated at the first resonant frequency of 3.55 GHz and the second resonant frequency of 5.72 GHz. Both sections have a return loss of -51.48 dB and -37.94 dB, respectively. This number is acceptable for WiMAX and WLAN operation. The antenna's intended frequencies at 3.5 GHz and 5.8 GHz are -31.70 dB and -22.00 dB, respectively.
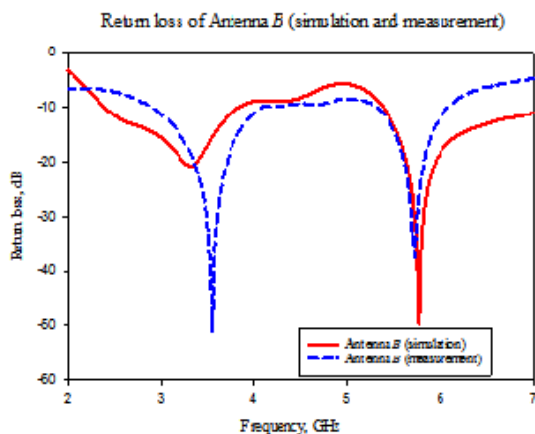

Fig. 12 comparison the measurement of Antenna *B* to its modelling

Table 2 represents Antenna *B*. It was discovered that the gain and directivity performance of this antenna was 2.23 dB and 2.43 dBi at the first resonant frequency point. However, the gain and directivity performance of the antenna were 2.83 dB and 3.85 dBi at the second resonant frequency.

Table 2: Performance results of Antenna *B*

Parameter	Antenna B sim	
Resonant frequency, f_r (GHz)	3.32	5.768
Return loss (dB)	- 20.826	- 49.556
Bandwidth (MHz), f_{High} - f_{Low} (GHz)	2.39 – 3.85	5.38 – 7.17
Gain (dB)	2.23	2.83
Directivity (dBi)	2.43	3.85

The distribution of electromagnetic power in free space was represented by the radiation pattern. The radiation pattern of the microstrip patch antenna for Antenna Design *B* is shown in Table 3 at 0^0 and 90^0. The primary lobe was discovered to radiate in the direction of 0^0 in the form of a nearly solid eight shape. For 90^0, it shows the nearly same with 0^0. Unlike the second resonant frequency, the eighth shape with large lobes toward the left direction and smaller lobes toward the right path is seen at = 0^0. This radiating pattern exhibits the butterfly-like shape for = 90^0.

The computed surface current of Antenna *B* at 0^0 and 90^0 are shown in Table 4. The current was focused on three different locations along the feedline, at the edge of the pentagonal patch and at the slot part. These two distinct phases of 0^0 and 90^0 revealed that they had nearly identical distribution flow situations.

Figure 14 shows the computed surface current of Antenna *B* at 0^0 and 90^0. The current was focused on three different locations along the feed line, at the edge of the

pentagonal patch, and at the slot part. These two distinct phases of 0^0 and 90^0 reveal that they have nearly identical distribution flow situations.
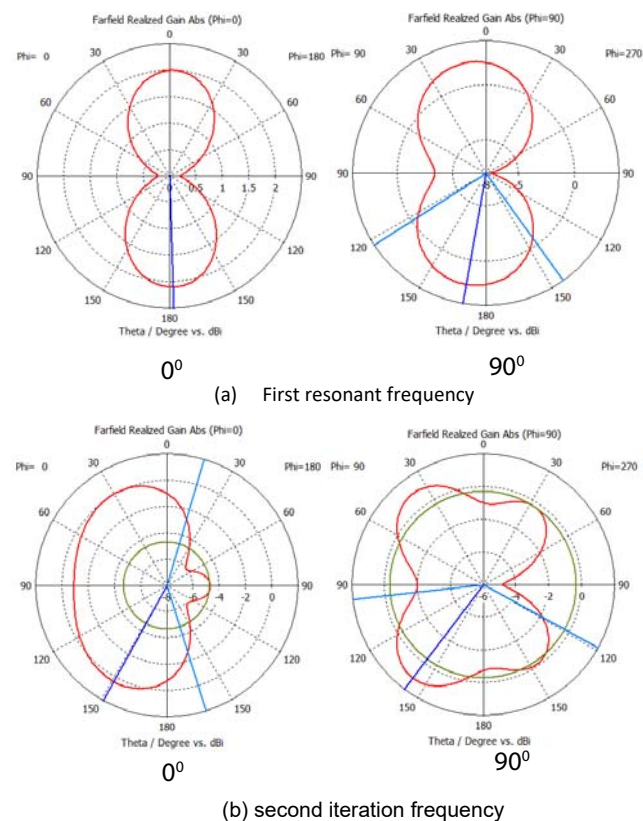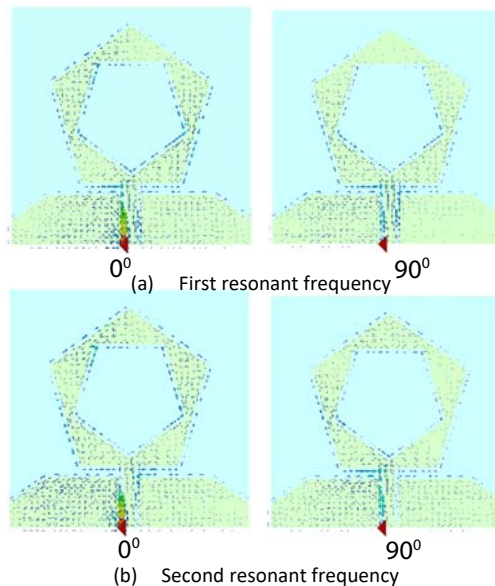

(a) First resonant frequency

(b) second iteration frequency

Fig. 13: Radiation pattern of Antenna *B* at $\phi = 0^0$ and $\phi = 90^0$ at the first and second resonant frequencies

(a) First resonant frequency

(b) Second resonant frequency

Fig/e 14: Surface current of Antenna *B* of phase 0^0 and 90^0 at the first and second resonant frequencies

Conclusion

This work presents the parametric analysis of a dual band CPW Pentagonal Sierpinski gasket fractal patch antenna for WLAN and WiMAX applications. In this work, five distinct parametric variables are used to define the impact of various antenna dimensions. The first Antenna *A* basic design, the first Antenna *B* iteration with a pentagonal shaped structure with the pentagonal slot, the results show that the position of the resonant frequency and the

performance of the proposed antenna are affected by modifying the initiator shape to the first iteration step of the pentagonal island structure. At wanted frequencies at 3.5 GHz and 5.8 GHz, the antenna's aimed frequencies are -31.70 dB and - 22.00 dB, respectively, and these values are feasible for WiMAX and WLAN operation. This claim is correspondingly valid with regard to the antenna design's inclusion of a small pentagonal shape.

REFERENCES

[1] M. R. C and R. Boopathi Rani, "A Compendious Review on Fractal Antenna Geometries in Wireless Communication," 2020 International Conference on Inventive Computation Technologies (ICICT), 2020, pp. 888-893

[2] N.-Y. Li, Z. Zakaria, N. Shairi, H. Alsariera, R. Alahnomi, Design and Investigation on Wideband Antenna based on Polydimethylsiloxane (PDMS) for Medical Imaging Application, Przegląd Elektrotechniczny, 3, 89 – 92

[3] M. Alibakhshikenari et al., Impedance Bandwidth Improvement of a Planar Antenna Based on Metamaterial-Inspired T-Matching Network, IEEE Access, 2021, 9, 67916-6792 DOI:10.1109/ACCESS.2021.3076975

[4] M. Alibakhshikenari, B. S. Virdee, V. Vadalà, M. Dalarsson, M. E. de C. Gómez, A. G. Alharbi, S. N. Burokur, S. Aïssa, I. Dayoub, F. Falcone, E. Limiti, Broadband 3-D shared aperture high isolation nine-element antenna array for on-demand millimeter-wave 5G applications, Optik, 2022, 267, 169708 DOI:10.1016/j.ijleo.2022.169708

[5] W. J. Krzysztofik, "Fractals in Antennas and Metamaterials Applications", in Fractal Analysis - Applications in Physics, Engineering and Technology. London, United Kingdom: IntechOpen, 2017

[6] V. M and V. R, "A Fractal Miniaturized Compact Antenna for V2X - 5G Communication," 2021 5th International Conference on Computer, Communication and Signal Processing (ICCCSP), 2021, pp. 1-4

[7] W. A. Awan, M. Alibakhshikenari and E. Limiti, "Design and Analysis of a Simple Miniaturized Fractal Antenna for 5G Ka-Band Applications," 2021 IEEE Asia-Pacific Microwave Conference (APMC), 2021, pp. 22-24

[8] Mandelbrot, B. B., Fractals: Form, Chance and Dimension, Freeman & Company, W. H., 1997

[9] B. B. Mandelbrot, The Fractal Geometry of Nature. San Francisco, CA: Freeman, 1983.

[10] A. Kumar, B. C. Sahoo, G. Singh and A. P. Singh, "Design of Micro-Machined Frequency Reconfigurable Cascaded Sierpinski Gasket Fractal Antenna using RF-MEMS Switches," 2021 IEEE MTT-S International Microwave and RF Conference (IMARC), pp. 1-4, 2021

[11] V. V. Reddy, E. Navyasri, Sreemeghana, P. Shashidhar and S. Faize, "Minkowski Fractal Boundary Patch Antenna for GPS Application," 2021 6th International Conference on Communication and Electronics Systems (ICCES), pp. 385-388, 2021

[11] X. Cao, B. Luo, Y. Zhu, Z. Xia and Q. Cai, "Research on the Defected Ground Structure with Von Koch Snowflake Fractals," in IEEE Access, vol. 8, pp. 32404-32411, 2020

[12] J. A. Russer, "Printed self-complementary Hilbert curve (SCHC) fractal broad-band antenna," 2018 Baltic URSI Symposium (URSI), pp. 206-209, 2018

[13] J. B. Benavides, R. A. Lituma, P. A. Chasi and L. F. Guerrero, "A Novel Modified Hexagonal Shaped Fractal Antenna with Multi Band Notch Characteristics for UWB Applications," 2018 IEEE-APS Topical Conference on Antennas and Propagation in Wireless Communications (APWC), 2018, pp. 830-833

[14] W. Sierpinski, "Sur une courbe dont tout point est un point de ramification," C. R. Acad., Paris 160 302, 1915.

[15] K. D, Purnomo, N. P. W. Sari, F. Ubaidillah, I. H. Agustin, The construction of the Koch curve (n,c) using L-system, AIP Conference Proceedings, 2022, 1, 1-8

[16] C. P. Baliarda, J. Romeu and A. Cardama, The Koch monopole: a small fractal antenna, in IEEE Transactions on Antennas and Propagation, 2000, 48, 11, 1773-1781 DOI: 10.1109/8.900236

[16] W. Sierpinski, Sur une courbe dont tout point est un point de ramification, C. R. Acad., Paris 160 302, 1915. DOI: 10.1063/1.5141721

[17] C. Puente-Baliarda and R. Pous, Fractal design of multiband and low side-lobe arrays, IEEE Transactions on Antennas and Propagation, 1996, 44, 5, 730 DOI: 10.1109/8.496259.

[18] E. M. Anitas, Structural Properties of Molecular Sierpiński Triangle Fractals, Nanomaterials, 2020, DOI: 10.3390/nano10050925

[19] Devcsh, M. G. Siddiqui, A. K. Saroj and J. A. Ansari, Performance analysis of Rotated Square Sierpinski Gasket (RSSG) fractal antenna for wireless communication, 2018 5th IEEE Uttar Pradesh Section International Conference on Electrical, Electronics and Computer Engineering (UPCON), 2018, 1-4 10.1109/UPCON.2018.8597125

[20] Y. B. Chaouche, M. Nedil, B. Hammache and M. Belazzoug, Design of Modified Sierpinski Gasket Fractal Antenna for Tri-band Applications, 2019 IEEE International Symposium on Antennas and Propagation and USNC-URSI Radio Science Meeting, 2019, 889-890 DOI: 10.1109/APUSNCURSINRSM.2019.8889038

[21] B. R. Franciscatto, T. P. Vuong and G. Fontgalland, High gain Sierpinski Gasket fractal shape antenna designed for RFID, 2011 SBMO/IEEE MTT-S International Microwave and Optoelectronics Conference (IMOC 2011), 2011, 239-243 DOI: 10.1109/IMOC.2011.6169374

[22] A. Gehani, P. Agnihotri and D. Pujara, Analysis and synthesis of sierpinski gasket fractal antenna using ANFIS, 2017 IEEE International Symposium on Antennas and Propagation & USNC/URSI National Radio Science Meeting, 2017, 353-354 DOI: 10.1109/APUSNCURSINRSM.2017.8072219

[23] S. Yikilmazcinar, E. Basaran and H. A. Ülkü, Single Fed UWB Sierpinski Fractal Monopole Antenna Array, 2019 Fifth International Electromagnetic Compatibility Conference (EMC Turkiye), 2019, 1-3 DOI: 10.1109/EMCTurkiye45372.2019.8976020

[24] J. Jayasinghe, A. Andújar, & J. Anguera, On the properties of Sierpinski gasket fractal microstrip antennas, Microwave and Optical Technology Letters, 2018, 1-5 DOI: 10.1002/mop.31605

[25] N. Jayarenjini and C. Unni, MERR Inspired CPW Fed SSGF Antenna for Multiband Operations, Progress in Electromagnetics Research C, 2019, 91, 197-211 DOI:10.2528/PIERC19020202

[26] V. Remya, M. Gajalakshmi, S. Jayashree and M. Kanthimathi, Low Profile Sierpinski Fractal Patch Antenna, 2022 International Conference on Communication, Computing, and Internet of Things (IC3IoT), 2022, 1-5 DOI: 10.1109/IC3IOT53935.2022.9767954

[27] A. K. Vallappil, M. K. A. Rahim, B. A. Khawaja and N. A. Murad, Metamaterial Sierpinski Carpet Antenna with Cross-Slot Superstrate for 5G Applications, 2021 IEEE International Symposium on Antennas and Propagation and USNC-URSI Radio Science Meeting (APS/URSI), 2021, 1964-1965 DOI: 10.1109/APS/URSI47566.2021.9704730